

The HARPS search for southern extra-solar planets*

XVII. Six long-period giant planets around BD-17 0063, HD 20868, HD 73267, HD 131664, HD 145377, HD 153950

C. Moutou¹, M. Mayor², G. Lo Curto³, S. Udry², F. Bouchy⁴, W. Benz⁵, C. Lovis², D. Naef³, F. Pepe², D. Queloz², and N.C. Santos⁶

¹ Laboratoire d'Astrophysique de Marseille, OAMP, Université Aix-Marseille & CNRS, 38 rue Frédéric Joliot-Curie, 13388 Marseille cedex 13, France
e-mail: Claire.Moutou@oamp.fr

² Observatoire de Genève, Université de Genève, 51 ch.des Maillettes, 1290 Sauverny, Switzerland.

³ ESO, Alonso de Cordoba 3107, Vitacura Casilla 19001, Santiago, Chile

⁴ Institut d'Astrophysique de Paris, 98bis bd Arago, 75014 Paris, France

⁵ Physikalischs Institut Universität Bern, Sidlerstrasse 5, 3012 Bern, Switzerland

⁶ Centro de Astrofísica, Universidade do Porto, Rua das Estrelas, 4150-762 Porto, Portugal

Received ; accepted

ABSTRACT

We report the discovery of six new substellar companions of main-sequence stars, detected through multiple Doppler measurements with the instrument HARPS installed on the ESO 3.6m telescope, La Silla, Chile. These extrasolar planets are orbiting the stars BD-17 0063, HD 20868, HD 73267, HD 131664, HD 145377, HD 153950. The orbital characteristics which best fit the observed data are depicted in this paper, as well as the stellar and planetary parameters. Masses of the companions range from 2 to 18 Jupiter masses, and periods range from 100 to 2000 days. The observational data are carefully analysed for activity-induced effects and we conclude on the reliability of the observed radial-velocity variations as of exoplanetary origin. Of particular interest is the very massive planet (or brown-dwarf companion) around the metal-rich HD 131664 with $m_2 \sin i = 18.15 M_{Jup}$ and a 5.34-year orbital period. These new discoveries reinforces the observed statistical properties of the exoplanet sample as known so far.

Key words. stars: individual: BD-17 0063, HD 20868, HD 73267, HD 131664, HD 145377, HD 153950 – stars: planetary systems – techniques: radial velocities – techniques: spectroscopic

1. Introduction

The HARPS¹ instrument (Pepe et al. 2003; Mayor et al. 2003) has been in operation since October 2003 on the 3.6m telescope in La Silla Observatory, ESO, Chile. It has allowed so far the discovery of several tens of extrasolar systems, among which very low-mass companions (e.g., Mayor et al. (2008)). The strategy of HARPS observations inside the Guaranteed Time Observation program is adapted to different target samples. High-precision is achieved on a sub-sample of bright stars, known to be stable at a high level. In addition, a larger, volume-limited sample of stars are being explored at a moderate precision (better than 3 m s^{-1} or signal-to-noise ratio of 40) in order to complete our view of exoplanets' properties with extended statistics. The HARPS sample completes the CORALIE sample with stars from 50 to 57.5 pc distance, and together, these samples contain about 2500 stars. The results presented in this paper concern this wide exploratory program at moderate precision. Earlier findings in this stellar sample consist in 8 giant planets, which have been presented in Pepe et al. (2004), Moutou et al. (2005), Lo Curto et al. (2006),

and Naef et al. (2007). The statistical properties of these planets encounter those described in the literature (Marcy et al. 2005; Udry & Santos 2007), regarding the frequency of planets and the distribution of their parameters.

We report the discovery of six new planets in the volume-limited sample of main-sequence stars, using multiple HARPS Doppler measurements over 3 to 5 years. They are massive and long-period planets. Section 2 describes the characteristics of the parent stars, and Section 3 presents the Doppler measurements and discusses the planetary orbital solutions.

2. Characteristics of the host stars

The host stars discussed here are: BD-17 0063, HD 20868, HD 73267, HD 131664, HD 145377, and HD 153950. We used the V magnitude and $B - V$ color index given in the HIPPARCOS catalog (ESA 1997), and the Hipparcos parallaxes π as recently reviewed by van Leeuwen (2007), to estimate the absolute magnitude M_V . The bolometric correction of Flower (1996) is then applied to recover the absolute luminosity of the stars.

Spectroscopic parameters T_{eff} , $\log g$, and $[Fe/H]$ were derived from a set of FeI and FeII lines (Santos et al. 2004) for which equivalent widths were derived with ARES (Automatic Routine for line Equivalent width in stellar Spectra, Sousa et al. (2007, 2008)) on the HARPS spectra. The error-bars reflect the

Send offprint requests to: C. Moutou

* Based on observations made with the HARPS instrument on the ESO 3.6 m telescope at La Silla Observatory under programme ID 072.C-0488(E).

¹ High-Accuracy Radial-velocity Planet Searcher

large number of FeI and FeII lines used, and a good precision is obtained, especially on the effective temperature. For gravity and metallicity estimates we are limited by systematics, which are included in the error bars.

We finally estimate the stellar mass and age, from T_{eff} , $[Fe/H]$, and parallax estimates, by using Padova models of Girardi et al. (2000) and its web interface as described in da Silva et al. (2006). Errors are propagated and estimated using the Bayesian method. The stellar radius is finally estimated from the simple relationship between luminosity, temperature and radius.

From the HARPS cross-correlation function, we may derive an estimate of the projected rotational velocity of the star, $vsini$. The measurement of the core reversal in the calcium H & K lines provides an estimate of the chromospheric activity $\log R'_{HK}$ (see method in Santos et al. (2000)). The error bars of this quantity include the scatter as well as some systematics; these are particularly large for the faintest and coolest stars, with typical signal-to-noise ratio of 10 in the region of the calcium doublet. All measured stellar parameters and their errors are given in Table 1. A short presentation of the host stars follows.

2.1. BD-17 0063, HD 20868, and HD 73267: three quiet K-G stars

BD-17 0063 is a main-sequence K5 and HD 20868 is slightly evolved K3/4 IV star. Both are slow rotators which do not exhibit a significant activity jitter. They have a metallicity compatible with the Sun metallicity and masses of respectively 0.74 and $0.78 M_{\odot}$ and estimated age of more than 4 Gyr. HD 73267 is somewhat more massive with $0.89 M_{\odot}$. It also shows no significant activity, rotates slowly and has a solar metallicity. It is a 7 Gyr-old G5 dwarf. **The rotation period of our sample stars can be extrapolated from the activity level using relations in Noyes et al. (1984) (colour to convection turnover time relations) and Mamajek & Hillenbrand (2008) (Rossby number to $\log R'_{HK}$ relations). We find rotation periods of 39, 51 and 42 days, respectively for BD-17 0063, HD 20868, and HD 73267.**

2.2. HD 131664, HD 145377, and HD 153950: two early G and one late F dwarf stars

The other three stars HD 131664, HD 145377, and HD 153950 are slightly more massive than the Sun with respectively 1.10, 1.12 and $1.12 M_{\odot}$. HD 145377 is the most active one and its age is estimated around 1 Gyr. Their rotational periods are also shorter than for the first group of lower mass stars, **with 22, 12 and 14 days respectively for HD 131664, HD 145377, and HD 153950**. HD 131664 and HD 145377 are both metal-rich stars with $[Fe/H] = 0.32$ and 0.12, respectively, while HD 153950 has a metallicity close to solar.

3. Radial velocity data and orbital solutions

3.1. BD-17 0063

We gathered 26 spectra of BD-17 0063 with HARPS over a timespan of 1760 days between October 31st 2003 and July 5th 2008. The mean radial-velocity uncertainty is 1.6 m s^{-1} . The measurements are given in Table 3 (electronic version only) and shown in Figure 1. We fitted a Keplerian orbit to the observed radial-velocity variations, and found a best solution with a period of 655.6 days. It is an eccentric orbit ($e = 0.54$) with a

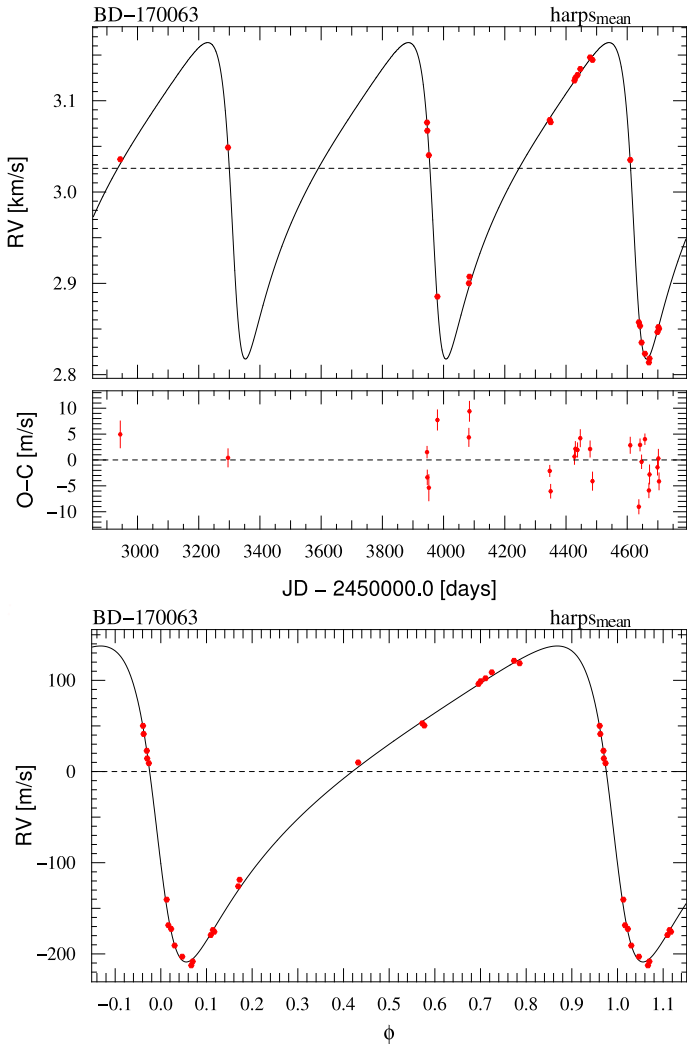


Fig. 1. The radial-velocity curve of BD-17 0063 obtained with HARPS. Top: individual radial-velocity measurements (dots) versus time, and fitted orbital solution (solid curve); Middle: residuals to the fitted orbit versus time; Bottom: radial-velocity measurements with phase-folding, using the period of 655.6 days and other orbital parameters as listed in Table 2. A $5.1 M_{Jup}$ companion to this K5 dwarf is evidenced.

semi-amplitude of 173 m s^{-1} . The reduced χ^2 obtained on this fit is 3.2.

The inverse bisector slope is estimated on the cross-correlation function and its timeseries is also examined, in order to exclude the stellar variability as origin of the observed radial-velocity variation (Queloz et al. 2001). The error on the bisector slope is taken as twice the error on the velocity, as a conservative value. No correlation is found between the bisector slope and the velocity, which excludes a blend scenario. The bisector values for BD-17 0063 are compatible with a constant value with a standard deviation of 7 m s^{-1} , over the 4.8 yr time span. With the long rotation period estimated for the star (39 days), a radial-velocity modulation related to spot activity is also very unprobable. These activity indicators thus strongly support the planetary origin of the observed signal.

With the stellar parameters as determined in the previous section, we infer a minimum planetary mass of $m_2 \sin i = 5.1$

Table 1. Observed and inferred stellar parameters for the planet-hosting stars presented in this paper.^a **The rotation periods of the stars are not derived from observations, but indirectly inferred from $\log R'_{\text{HK}}$ with relationships in Mamajek & Hillenbrand (2008) and Noyes et al. (1984).**

Parameter	BD-17 0063	HD 20868	HD 73267	HD 131664	HD 145377	HD 153950
Sp	K5V	K3/4IV	G5V	G3V	G3V	F8V
V	[mag]	9.62	9.92	8.90	8.13	8.12
$B - V$	[mag]	1.128	1.037	0.806	0.667	0.623
π	[mas]	28.91 (1.27)	20.42 (1.38)	18.21 (0.93)	18.04 (0.73)	18.27 (0.94)
d	[pc]	34.6 (1.5)	48.9 (3.5)	54.91 (3.0)	55.43 (2.3)	57.7 (3.0)
M_V	[mag]	6.92	6.47	5.20	4.41	4.31
$B.C.$	[mag]	-0.49	-0.41	-0.195	-0.08	-0.055
L	[L_\odot]	0.21 (0.02)	0.296 (0.04)	0.783 (0.09)	1.46 (0.13)	1.56 (0.17)
T_{eff}	[K]	4714 (93)	4795 (124)	5317 (34)	5886 (21)	6046 (15)
$\log g$	[cgs]	4.26 (0.24)	4.22 (0.26)	4.28 (0.1)	4.44 (0.1)	4.49 (0.1)
[Fe/H]	[dex]	-0.03 (0.06)	0.04 (0.1)	0.03 (0.02)	0.32 (0.02)	0.12 (0.01)
M_*	[M_\odot]	0.74 (0.03)	0.78 (0.03)	0.89 (0.03)	1.10 (0.03)	1.12 (0.03)
$v \sin i$	[km s^{-1}]	1.5	1.1	1.65	2.9	3.85
$\log R'_{\text{HK}}$		-4.79 (0.1)	-4.99 (0.1)	-4.97 (0.07)	-4.82 (0.07)	-4.62 (0.04)
$P_{\text{rot}}(\text{HK})^a$	[days]	39	51	42	22	12
Age	[Gy]	4.3 (4)	4.5 (4)	7.4 (4.5)	2.4 (1.8)	1.3 (1)
R_*	[R_\odot]	0.69	0.79	1.04	1.16	1.14
						1.34

M_{Jup} and semi-major axis of 1.34 AU. The periastron distance is 0.87 AU which infers a transit probability of only 0.4%. No attempt was made yet to monitor the photometric lightcurve of BD-17 0063 nor to search for a potential transit. Figure 1 shows the radial-velocity signal folded with the planetary phase and the residuals against time when the main signal is subtracted. There is no significant periodic trend nor linear drift in the O-C residuals, with a standard deviation of 4.1 m s^{-1} , i.e., marginally above the individual errors. All parameters of the orbit and the planet are given in Table 2, together with their estimated error.

3.2. HD 20868

Observations of HD 20868 consist in 48 HARPS measurements obtained over 1705 days between November 1st 2003 and July 2nd 2008. The mean uncertainty on the radial velocity measurements is 1.5 m s^{-1} . The measurements are given in Table 4 (electronic version only). Figure 2 shows the velocities as a function of time, as well as the Keplerian orbit with a period of 380.85 days that best fits the data. The residual values, after subtraction of the fit, are also shown against time. There is no significant trend in these residuals, characterized by a standard deviation of 1.7 m s^{-1} . The reduced χ^2 of the fit is 1.27.

The best orbital solution is a strongly eccentric orbit ($e = 0.75$) with a semi-amplitude of 100.34 m s^{-1} . The inferred minimum mass of the companion responsible for this velocity variation is $1.99 M_{Jup}$ and a semi-major axis of 0.947 AU is derived from the third Kepler law. The periastron distance is 0.54 AU which corresponds to a transit probability of 0.7%.

The bisector test was applied and excludes that the velocity variations are due to stellar activity. A trend which is confirmed by the long rotation period.

3.3. HD 73267

We gathered 39 HARPS measurements of HD 73267 over a time span of 1586 days, from November 27th 2004 and May 31st 2008. Small individual uncertainties are obtained, with a mean value of 1.8 m s^{-1} . Data are shown in Table 8 and in Figure 3. The observed velocity variations were fitted with a Keplerian orbit. The best solution corresponds to a period of 1260 days,

eccentricity of 0.256 and semi-amplitude of 64.29 m s^{-1} . The scatter of the residuals is compatible with the radial-velocity uncertainty and these residuals show no specific trend. The $O - C$ standard deviation is 1.7 m s^{-1} and reduced χ^2 is 1.19.

The bisector variations are not correlated to the velocity variations nor in phase with the signal, which excludes the stellar variability as being the cause of it. Here again, the estimated rotation period of the star is long, and spot-related activity cannot be considered as a potential origin for the observed signal.

The minimum mass of the inferred companion is $3.06 M_{Jup}$ and a semi-major axis of 2.198 AU is calculated for this 3.44 year period companion.

3.4. HD 131664

We gathered 41 measurements of HD 131664 over 1463 days with HARPS, from May 21st 2004 and May 23rd 2008. Individual uncertainties have a mean value of 2 m s^{-1} . A long-term velocity variation is observed (Figure 4), which is best fitted with a Keplerian orbit of 1951 days, 0.638 eccentricity and a large semi-amplitude K of 359.5 m s^{-1} . The residuals after subtraction of this signal have a standard deviation of only 4 m s^{-1} and no specific trend. The reduced χ^2 of the fit is 2.97. **Although the orbital fit to the data appears robust, the time coverage of this planetary orbit is not perfect, as most of the periastron passage has unfortunately been missed. This limits the precision we get on the orbital parameters.**

The bisector test again confirms the origin of this signal as due to a sub-stellar companion. The large amplitude despite the long period of the signal results in a large projected mass of the companion, i.e. $m_2 \sin i = 18.15 M_{Jup}$. This massive planet, or brown-dwarf companion, orbits the parent star at a semi-major axis of 3.17 AU.

3.5. HD 145377

We gathered 64 measurements of HD 145377 with HARPS from June 21st 2005 to July 1st 2008, over 1106 days. A mean uncertainty of 2.3 m s^{-1} is obtained. A relatively large-amplitude velocity variation is observed, as shown in Figure 5. It is best fitted with a 103.95 day period. The orbit is eccentric ($e = 0.307$)

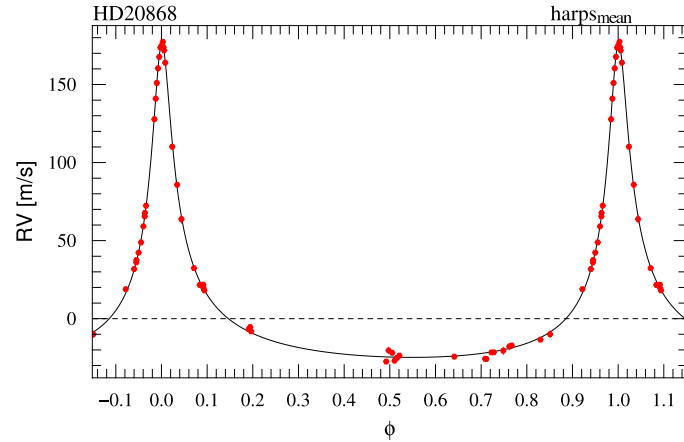
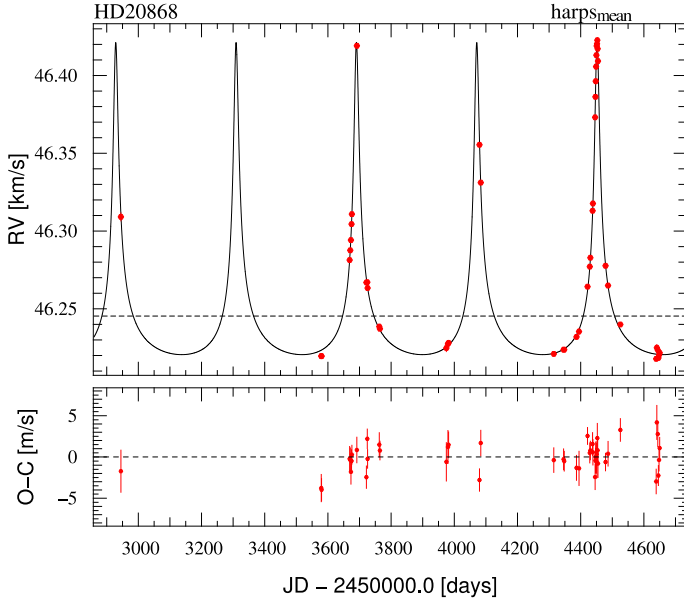


Fig. 2. The radial-velocity curve of HD 20868 obtained with HARPS. Top: individual radial-velocity measurements (dots) versus time, and fitted orbital solution (solid curve); Middle: residuals to the fitted orbit versus time; Bottom: radial-velocity measurements with phase-folding, using the period of 380.85 days and other orbital parameters as listed in Table 2. The K3/4 IV star has a $1.99 M_{Jup}$ companion.

and semi-amplitude $K = 242.7 \text{ m s}^{-1}$. Although the signal is very clear and stable over more than 10 periods, the residuals to the fit are affected by an additional jitter, of amplitude 15.3 m s^{-1} . This jitter was expected from the relatively young age (1 Gyr) and the high value of $\log R'_{HK}$ (mean value is -4.68), which strongly suggests that stellar variability is observed in addition to the main signal. The O-C residuals do not show, however, a periodicity **related to the 12d rotation**, which is not surprising over about 80 rotation cycles of the star. **The Lomb-Scargle periodogram of the residuals do show, however, a tendency for a curved drift that could be a hint for a second, longer-period planet, and other periodic signals could be present but too weak to be significant.** When taken into account, the curved drift decreases the residual noise from 15 to about 10 m s^{-1} . **More data in the future may therefore reveal more planets in this system, but the present material is not conclusive in this respect.**

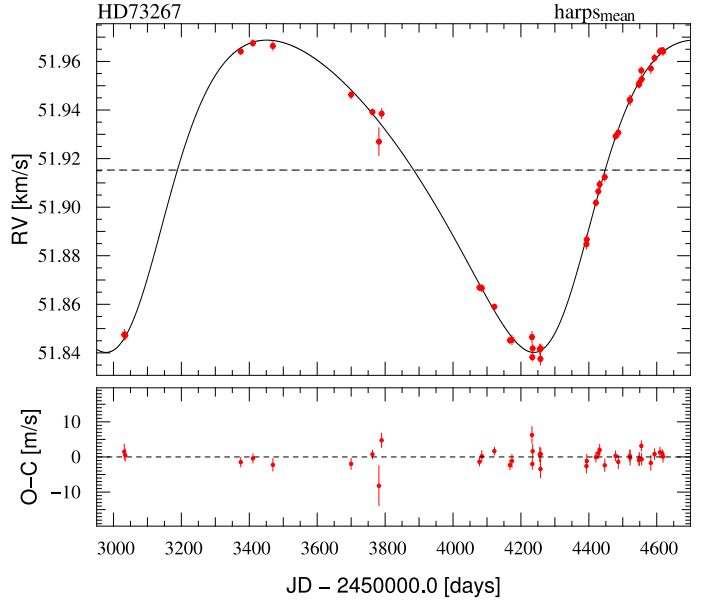


Fig. 3. The radial-velocity curve of HD 73267 obtained with HARPS. Top: individual radial-velocity measurements (dots) versus time, and fitted orbital solution (solid curve). The star has a companion of minimum mass $3.06 M_{Jup}$ and orbital period 1260 days. Bottom: residual to the fitted orbit versus time.

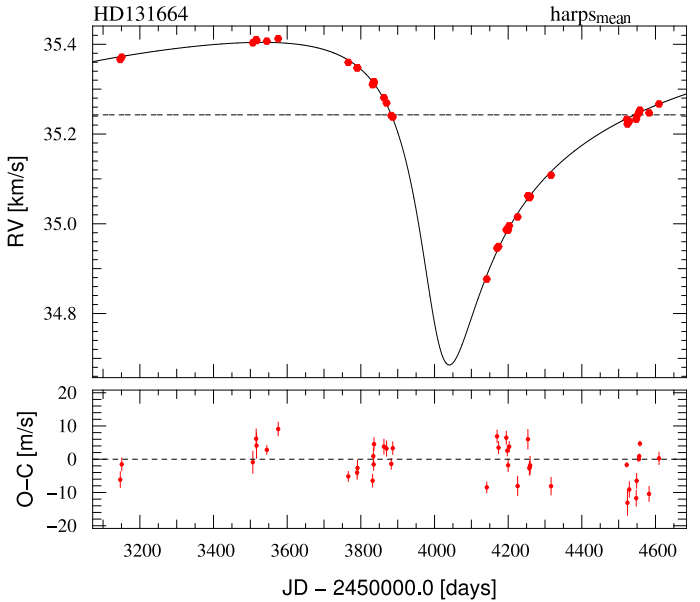


Fig. 4. The radial-velocity curve of HD 131664 obtained with HARPS. Top: individual radial-velocity measurements (dots) versus time, and fitted orbital solution (solid curve). It shows a very massive planetary companion of $m_2 \sin i = 18.15 M_{Jup}$ with an orbital period of 1951 days. Bottom: residual to the fitted orbit versus time.

Figure 6 shows the bisector behaviour with respect to radial velocity (top) and as a function of the fit residuals. The scatter of the bisector span is larger than for the other stars, with a value of 11 m s^{-1} , and it confirms that we see some line profile variations with time. The bisector slope does not correlate, however, with the radial velocity, excluding the stellar variability to be the only

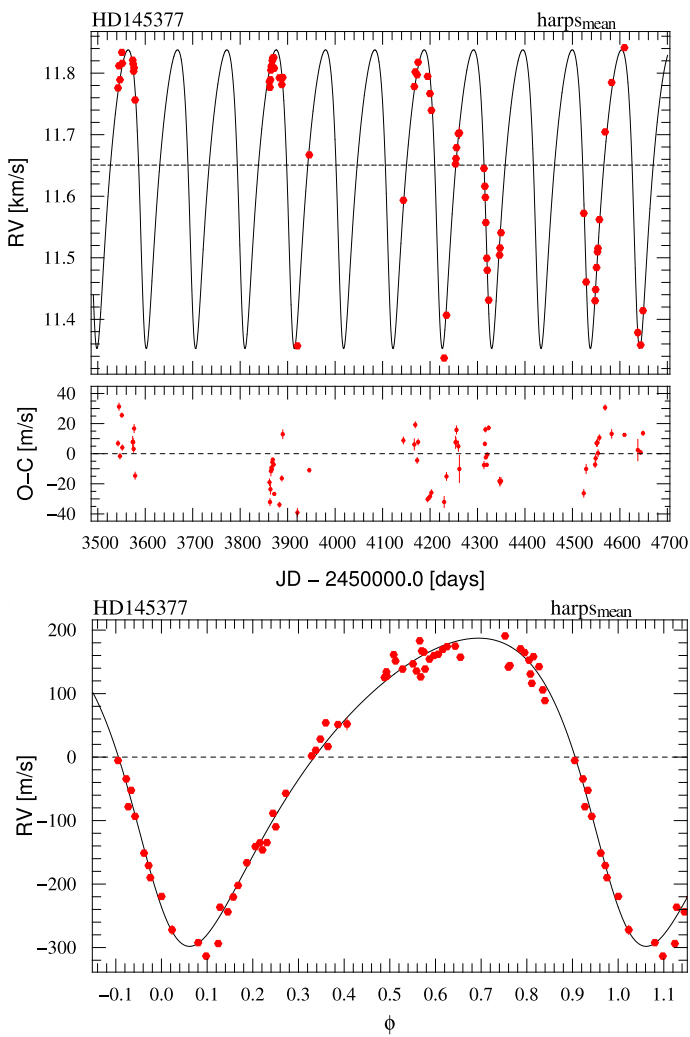


Fig. 5. The radial-velocity curve of HD 145377 obtained with HARPS. Top: individual radial-velocity measurements (dots) versus time, and fitted orbital solution (solid curve); Middle: residuals to the fitted orbit versus time; Bottom: radial-velocity measurements with phase-folding, using the period of 103.95 days and other orbital parameters as listed in Table 2. The residual jitter is due to stellar variability (expected from activity indicators) and shows no periodic trend. A planet of minimum mass $5.76 M_{Jup}$ is evidenced.

origin of the observed velocity variation. We also find no correlation between the residuals to the fitted orbit and the bisector span (Figure 6 bottom). Such a correlation, observed when the activity is mainly related to spots, could have been used to correct the radial velocities for stellar variability, as explained in Melo et al. (2007). Finally, as a test to the origin of the RV jitter, we observed HD 145377 in a sequence of 10 consecutive 90s exposures, for which a standard deviation of 2.5 m s^{-1} is derived. The stellar jitter therefore does not come from short-term acoustic modes but rather from chromospheric activity features.

The planetary companion of HD 145377 is a $m_2 \sin i = 5.76 M_{Jup}$ planet orbiting with a 103.95d period. The semi-major axis is 0.45 AU. The periastron distance is 0.34 AU which corresponds to a transit probability of 0.14%.

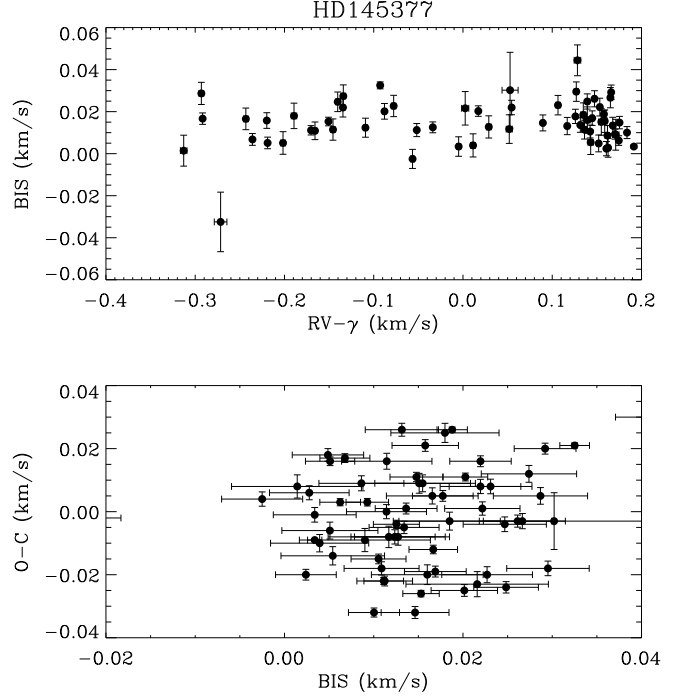


Fig. 6. The inverse bisector slope is plotted against the radial velocity of HD 145377 (top) and against the residuals to the fitted orbit (bottom). No correlation between these quantities is observed. Although the bisector varies in a similar scale as the fit residuals, we cannot correct for spot-related activity. The amplitude of bisectors' variations still remains small compared to the range of radial velocities.

3.6. HD 153950

Finally, the star HD 153950 was observed 49 times with HARPS from August 1st 2003 to June 26th 2008 (1791 day time span). The mean uncertainty of the velocity measurements is 2 m s^{-1} . The velocity variation with time is fitted with a Keplerian orbit of 499.4 day period (Figure 7). It is again an eccentric orbit with $e = 0.34$ and a semi-amplitude of 69.15 m s^{-1} . The bisector is rather flat over time and does not correlate with the orbital phase nor the position of the velocity peak. The residuals around the best solution have a standard deviation of 4 m s^{-1} and the reduced χ^2 obtained for the fit is 2.40.

This radial-velocity curve thus shows a planetary companion of minimum mass $2.73 M_{Jup}$. Its semi-major axis is 1.28 AU.

The orbit and planetary parameters of the six new systems described above are given with their inferred errors in Table 2.

4. Conclusion

From long-term observations with HARPS with individual uncertainty around 2 m s^{-1} , we were able to derive the presence of 6 new substellar companions around the main-sequence stars BD-17 0063, HD 20868, HD 73267, HD 131664, HD 145377, and HD 153950.

The analysis of the HARPS cross-correlation function and in particular the bisector span of each measurement, allows to discard long-term stellar variability as the origin of the observed radial-velocity curve. This proved efficient even for the most active star, HD 145377: characterizing the planetary companion

Table 2. Orbital and physical parameters for the planets presented in this paper. T is the epoch of periastron. $\sigma(O-C)$ is the residual noise after orbital fitting of the combined set of measurements. χ^2_{red} is the reduced χ^2 of the fit.

Parameter	BD-17 0063 b	HD 20868 b	HD 73267 b	HD 131664 b	HD 145377 b	HD 153950 b
P [days]	655.6 (0.6)	380.85 (0.09)	1260. (7)	1951. (41)	103.95 (0.13)	499.4 (3.6)
T [JD-2400000]	54627.1 (1.5)	54451.52 (0.1)	51821.7 (16)	52060. (41)	54635.4 (0.6)	54502. (4.3)
e	0.54 (0.005)	0.75 (0.002)	0.256 (0.009)	0.638 (0.02)	0.307 (0.017)	0.34 (0.021)
γ [km s $^{-1}$]	3.026 (0.0012)	46.245 (0.0003)	51.915 (0.0005)	35.243 (0.004)	11.650 (0.003)	33.230 (0.001)
ω [deg]	112.2 (1.9)	356.2 (0.4)	229.1 (1.8)	149.7 (1.0)	138.1 (2.8)	308.2 (2.4)
K [m s $^{-1}$]	173.3 (1.7)	100.34 (0.42)	64.29 (0.48)	359.5 (22.3)	242.7 (4.6)	69.15 (1.2)
$a_1 \sin i$ [10 $^{-3}$ AU]	8.76	2.305	7.196	49.678	2.2074	2.981
$f(m)$ [10 $^{-9}$ M $_{\odot}$]	209.0	11.26	31.324	4295.665	132.788	14.174
$m_2 \sin i$ [M $_{Jup}$]	5.1 (0.12)	1.99 (0.05)	3.06 (0.07)	18.15 (0.35)	5.76 (0.10)	2.73 (0.05)
a [AU]	1.34 (0.02)	0.947 (0.012)	2.198 (0.025)	3.17 (0.03)	0.45 (0.004)	1.28 (0.01)
N_{meas}	26	48	39	41	64	49
S_{pan} [days]	1760	1705	1586	1463	1106	1791
$\sigma(O-C)$ [m s $^{-1}$]	4.1	1.7	1.7	4.0	15.3	3.9
χ^2_{red}	3.2	1.27	1.19	2.97	10.13	2.40

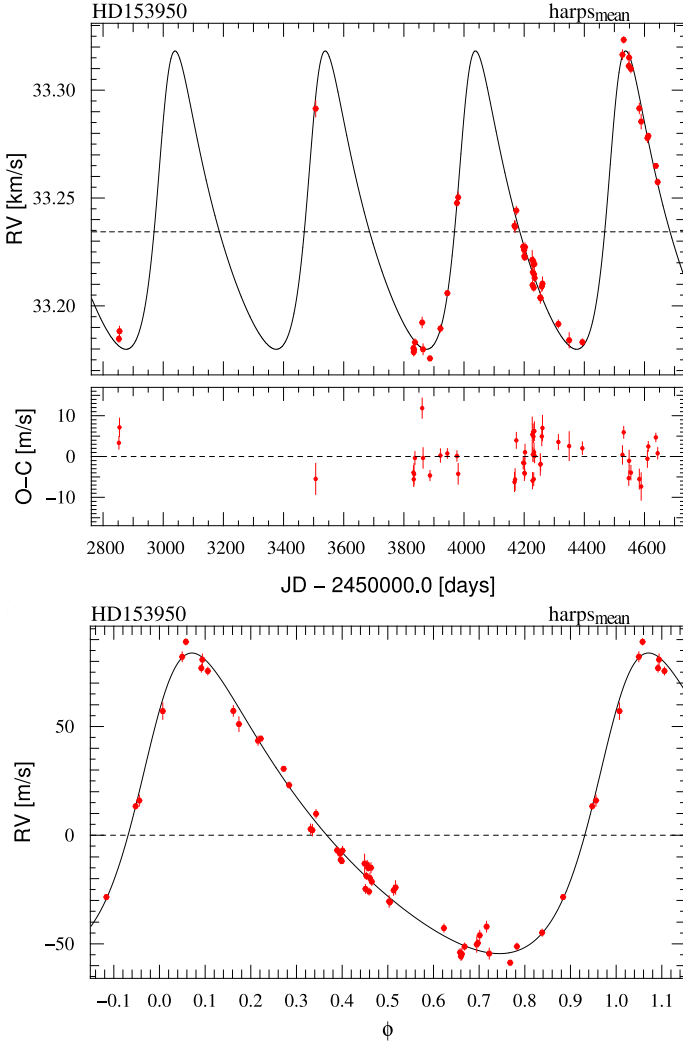


Fig. 7. The radial-velocity curve of HD 153950 obtained with HARPS. Top: individual radial-velocity measurements (dots) versus time, and fitted orbital solution (solid curve); Middle: residuals to the fitted orbit versus time; Bottom: radial-velocity measurements with phase-folding, using the period of 499.4 days and other orbital parameters as listed in Table 2. The planetary companion has a minimum mass of 2.73 M $_{Jup}$.

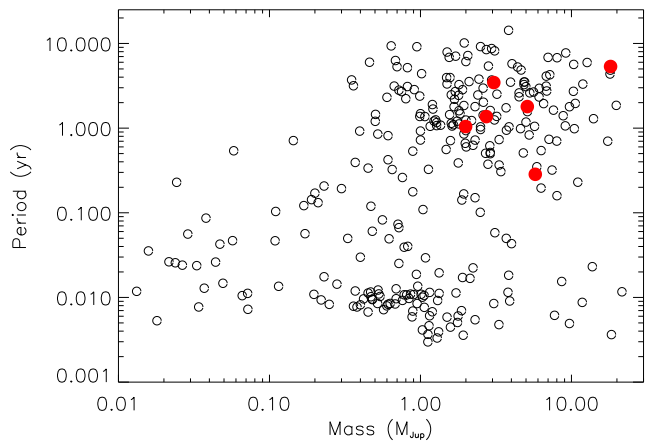


Fig. 8. The present mass-period diagram of known exoplanets (open circles) showing the location of the six new planets presented in this paper (filled circles). They belong to the bulge of the most massive, longest period bodies.

does not suffer too much from the stellar variability, because of the planet's relatively short period with respect to our long time span of observations (104 versus 1106 days). The stellar activity here translates into a residual jitter that does not hide the planet's signal.

The planet orbiting HD 131664 is very massive, with a minimum mass of 18.15 M $_{Jup}$, over the deuterium limit. It has characteristics similar to the other massive planet in distant orbit HD 168443 c (Udry et al. 2002), except that no internal planet to the system of HD 131664 is evidenced so far. The period of HD 131664 b (1951 days or 5.34 years) is also among the dozen longest known so far. Depending on the actual system age of HD 131664, the magnitude difference with the parent star could be as low as 13.5 in the K band – for the lower edge of the age range – and up to 20, using the models of Baraffe et al. (2002) for luminosity estimates. The angular separation ranges from 0.035 to 0.16 arcsec during the orbit. Depending on the system's inclination – and thus the true mass of the companion – it may be a target for future direct imaging investigations, that would permit a better characterisation of this unusual system. Note also that the parent star is particularly metal-rich ([Fe/H] = 0.32) in comparison with the mean metallicity of the solar neighbourhood.

The rare combination of parameters for this system – companion's mass, orbital period, star's metallicity – could make it one important piece of constraints for theories of planetary formation. Getting astrometric measurements of the six new systems with VLTI/PRIMA would probably be possible, in order to better constrain their true mass.

The new planets discussed in this paper are part of the bulge of long period, massive extrasolar planets in eccentric orbits, with masses in the range $2\text{--}6 M_{Jup}$ and periods of 0.3 to 5.3 years. Their properties can be discussed in the frame of the statistical studies performed in well-defined stellar samples as in the ELODIE, CORALIE, or Lick+Keck+AAT surveys (see Marcy et al. (2005) and Udry & Santos (2007) for in-depth discussions):

- Giant gaseous planets are found around about 6-7% of known main-sequence stars, with semi-major axes up to about 5 AU. These six new planets contribute to increase the number of known systems, with today 15 planets over the 850 stars of the volume-limited sample monitored by HARPS. The 1.8% frequency of planet occurrence in this sample where observations started in 2003, is, however, not yet at the level of the oldest surveys. Identically, only five hot Jupiters were discovered in our sample, representing a frequency of 0.6%, to be compared to 1.2% frequency for more complete surveys. The new planet sample presented in this paper yet contains the longest periods found in this specific survey, with measurements obtained at the earliest ages of HARPS operations (Figure 8).
- The distribution of planet masses currently favors the small masses, despite the strong observational bias towards massive planets. Here we bring new evidence for planets in the highest mass edge, with minimum masses of 2 to $18 M_{Jup}$ (Figure 8).
- The period and eccentricity properties of the six new planets confirms the global tendency of very dispersed eccentricities beyond the circularization zone due to tidal interactions, compared to the circular orbits of giant and distant planets in the Solar System. The origin of such dispersed eccentricities remains a mystery despite a number of theoretical attempts to match the observed distribution from a variety of eccentricity-damping physical processes.
- Host stars of systems with giant gaseous planets are significantly more metal-rich than average (Santos et al. 2005; Fischer & Valenti 2005), which is not debated by the new exoplanet sample presented here, with two stars having an excess metallicity compared to the Sun and no metal-poor planet-host star.
- About 12% of systems with gaseous giant planets are multiple. Here, we find no indication for a second body in any of the new systems, with a very small scatter of the residuals of the order of a few $m s^{-1}$ (except for HD 145377 which is active). In order to find planets of lower mass in these systems, a high-precision strategy should now be applied. Finding larger distance planets in these systems is also possible, although no significant long-term drift is yet observed.
- Finally, the mass-period distribution of the six new planets corroborates with the more general properties that more massive planets have longer orbital distances (e.g., Udry & Santos (2007)).

Adding new extrasolar systems to the ~ 300 planets known so far is of course of great importance to better characterize their properties. Radial-velocity survey, as well as transit-search programs, suffer the observational bias of detecting more easily the

short-period and massive planets -the rarest ones-, which may be the reason why only 6-7% of planets in the solar neighbourhood show the signature of a giant planet. Note that this proportion of stars with planetary systems greatly increases when planets in the mass range of Neptune or below are discovered (Mayor & Udry 2008). Extending the planet sample, especially in well-defined volume-limited samples of main-sequence stars as monitored by HARPS, is one of the new challenges of this scientific field, to help understanding the mechanisms which form and maintain planets around other stars.

Acknowledgements. N.C.S. would like to thank the support from Fundação para a Ciência e a Tecnologia, Portugal, through programme Ciência 2007 (C2007-CAUP-FCT/136/2006). We are grateful to the ESO staff for their support during observations.

References

Baraffe, I., Chabrier, G., Allard, F., & Hauschildt, P. H. 2002, A&A, 382, 563
 da Silva, L., Girardi, L., Pasquini, L., et al. 2006, A&A, 458, 609
 ESA. 1997, VizieR Online Data Catalog, 1239, 0
 Fischer, D. A. & Valenti, J. 2005, ApJ, 622, 1102
 Flower, P. J. 1996, ApJ, 469, 355
 Girardi, L., Bressan, A., Bertelli, G., & Chiosi, C. 2000, A&AS, 141, 371
 Lo Curto, G., Mayor, M., Clausen, J. V., et al. 2006, A&A, 451, 345
 Mamajek, E. E. & Hillenbrand, L. A. 2008, ArXiv e-prints
 Marcy, G., Butler, R. P., Fischer, D., et al. 2005, Progress of Theoretical Physics Supplement, 158, 24
 Mayor, M., Pepe, F., Queloz, D., et al. 2003, The Messenger, 114, 20
 Mayor, M. & Udry, S. 2008, in Nobel Symposium proceedings T 130, 014010
 Mayor, M., Udry, S., Lovis, C., et al. 2008, A&A, in press, astro-ph/0806.4587
 Melo, C., Santos, N. C., Gieren, W., et al. 2007, A&A, 467, 721
 Moutou, C., Mayor, M., Bouchy, F., et al. 2005, A&A, 439, 367
 Naef, D., Mayor, M., Benz, W., et al. 2007, A&A, 470, 721
 Noyes, R. W., Hartmann, L. W., Baliunas, S. L., Duncan, D. K., & Vaughan, A. H. 1984, ApJ, 279, 763
 Pepe, F., Mayor, M., Queloz, D., et al. 2004, A&A, 423, 385
 Pepe, F., Rupprecht, G., Avila, G., et al. 2003, in SPIE, 4841, 1045, 1045
 Queloz, D., Henry, G. W., Sivan, J. P., et al. 2001, A&A, 379, 279
 Santos, N. C., Israelian, G., & Mayor, M. 2004, A&A, 415, 1153
 Santos, N. C., Israelian, G., Mayor, M., et al. 2005, A&A, 437, 1127
 Santos, N. C., Mayor, M., Naef, D., et al. 2000, A&A, 361, 265
 Sousa, S. G., Santos, N. C., Israelian, G., Mayor, M., & Monteiro, M. J. P. F. G. 2007, A&A, 469, 783
 Sousa, S. G., Santos, N. C., Mayor, M., et al. 2008, A&A, 487, 373
 Udry, S., Mayor, M., Naef, D., et al. 2002, A&A, 390, 267
 Udry, S. & Santos, N. C. 2007, ARA&A, 45, 397
 van Leeuwen, F. 2007, A&A, 474, 653

Online Material

Table 3. Radial velocity values for BD -17 0063.

JD-2,400,000.	Radial Vel. [km s ⁻¹]	Uncertainty [km s ⁻¹]
52943.610509	3.03585	0.00258
53295.753206	3.04876	0.00174
53945.903440	3.07611	0.00111
53946.823277	3.06712	0.00141
53951.864680	3.04030	0.00252
53979.874025	2.88551	0.00194
54082.599768	2.90011	0.00174
54084.574580	2.90735	0.00192
54346.836046	3.07882	0.00107
54349.792760	3.07641	0.00132
54427.598625	3.12206	0.00149
54430.603057	3.12502	0.00140
54437.605063	3.12820	0.00137
54446.614295	3.13480	0.00164
54478.592373	3.14747	0.00155
54486.529176	3.14468	0.00174
54609.910593	3.03512	0.00155
54637.911547	2.85740	0.00136
54641.924906	2.85339	0.00115
54646.887252	2.83517	0.00130
54657.823636	2.82295	0.00101
54670.790307	2.81336	0.00139
54672.838582	2.81770	0.00183
54698.807055	2.84664	0.00149
54701.823517	2.85211	0.00177
54703.858883	2.85025	0.00162

Table 4. Radial velocity values for HD 20868.

JD-2400000.	Radial Vel. [km s ⁻¹]	Uncertainty [km s ⁻¹]
52944.759761	46.30911	0.00255
53578.941288	46.21963	0.00165
53579.927242	46.21953	0.00135
53668.773536	46.28134	0.00150
53670.728503	46.28763	0.00145
53672.797736	46.29419	0.00148
53674.743782	46.30446	0.00135
53675.819517	46.31087	0.00114
53691.577515	46.41910	0.00155
53721.706478	46.26692	0.00135
53724.633943	46.26712	0.00118
53725.585119	46.26338	0.00113
53762.579524	46.23860	0.00145
53764.539118	46.23716	0.00113
53974.869681	46.22482	0.00232
53979.923748	46.22749	0.00200
53981.897310	46.22813	0.00155
54079.673981	46.35546	0.00135
54083.717877	46.33114	0.00154
54314.874429	46.22101	0.00149
54345.833998	46.22372	0.00126
54347.832433	46.22375	0.00119
54386.726662	46.23193	0.00151
54394.752760	46.23539	0.00207
54421.692913	46.26423	0.00102
54428.736985	46.27712	0.00121
54430.633523	46.28286	0.00112
54437.676734	46.31306	0.00138
54438.644277	46.31772	0.00154
54445.632867	46.37310	0.00152
54446.708327	46.38629	0.00149
54447.647299	46.39631	0.00173
54448.662135	46.40572	0.00191
54449.673081	46.41303	0.00144
54450.625557	46.41899	0.00131
54451.657624	46.42038	0.00175
54452.629288	46.42265	0.00178
54453.668760	46.41719	0.00140
54454.671103	46.40928	0.00169
54478.640303	46.27767	0.00106
54486.573877	46.26497	0.00149
54525.518526	46.23992	0.00137
54638.948171	46.21787	0.00149
54640.934733	46.22498	0.00206
54643.941030	46.22350	0.00151
54645.930747	46.21843	0.00121
54647.933071	46.22028	0.00133
54649.925384	46.22170	0.00129

Table 5. Radial velocity values for HD 73267.

JD-2400000.	Radial Vel. [km s ⁻¹]	Uncertainty [km s ⁻¹]
53031.730610	51.84750	0.00214
53034.625318	51.84718	0.00171
53374.800416	51.96412	0.00131
53410.705484	51.96753	0.00130
53469.507660	51.96638	0.00175
53699.856836	51.94628	0.00153
53762.700039	51.93917	0.00120
53781.723770	51.92696	0.00565
53789.716242	51.93850	0.00202
54077.853694	51.86690	0.00117
54084.808437	51.86669	0.00154
54121.750283	51.85900	0.00107
54167.636520	51.84519	0.00134
54173.606470	51.84531	0.00188
54232.560360	51.84650	0.00231
54233.545820	51.83822	0.00148
54234.516188	51.84184	0.00191
54255.451119	51.84149	0.00207
54257.498753	51.83751	0.00248
54258.452112	51.84183	0.00170
54392.856053	51.88474	0.00192
54393.861259	51.88672	0.00183
54420.846468	51.90180	0.00134
54427.833648	51.90648	0.00148
54431.832778	51.90942	0.00157
54446.853818	51.91236	0.00172
54478.822609	51.92923	0.00138
54486.729809	51.93068	0.00185
54520.667295	51.94426	0.00167
54521.641787	51.94405	0.00208
54547.580289	51.95049	0.00144
54548.606686	51.95113	0.00184
54554.625472	51.95626	0.00146
54555.617466	51.95268	0.00161
54582.554316	51.95708	0.00209
54593.487209	51.96142	0.00148
54609.467804	51.96419	0.00142
54616.504677	51.96460	0.00111
54618.463621	51.96406	0.00157

Table 6. Radial velocity values for HD 131664.

JD-2400000.	Radial Vel. [km s ⁻¹]	Uncertainty [km s ⁻¹]
53146.689878	35.36621	0.00235
53150.721130	35.37138	0.00194
53506.661928	35.40323	0.00328
53515.682762	35.41041	0.00291
53516.706183	35.40838	0.00380
53544.650439	35.40707	0.00129
53575.529526	35.41260	0.00204
53765.883247	35.35969	0.00148
53789.862142	35.34722	0.00200
53790.891695	35.34791	0.00234
53831.878129	35.30995	0.00191
53833.894708	35.31519	0.00251
53834.793072	35.31172	0.00179
53835.766752	35.31675	0.00192
53862.689370	35.28105	0.00222
53869.760171	35.26920	0.00226
53882.633600	35.24120	0.00160
53886.645454	35.23779	0.00189
54141.891213	34.87671	0.00160
54169.833067	34.94571	0.00186
54173.842331	34.94933	0.00183
54194.919509	34.98657	0.00194
54197.764290	34.98699	0.00156
54199.875525	34.98575	0.00186
54202.767256	34.99557	0.00155
54225.722932	35.01516	0.00291
54253.647281	35.06246	0.00292
54257.633280	35.05809	0.00203
54258.634595	35.05959	0.00167
54259.617251	35.06109	0.00270
54316.466834	35.10819	0.00261
54521.868941	35.23283	0.00061
54523.843516	35.22223	0.00376
54528.845576	35.22825	0.00232
54547.737400	35.23304	0.00236
54548.830829	35.23871	0.00222
54554.803145	35.24746	0.00060
54555.817248	35.24875	0.00060
54557.770244	35.25325	0.00071
54582.619078	35.24712	0.00222
54609.613271	35.26701	0.00185

Table 7. Radial velocity values for HD 145377.

JD-2400000.	Radial Vel. [km s ⁻¹]	Uncertainty [km s ⁻¹]
53542.633832	11.77595	0.00170
53544.730958	11.81187	0.00238
53546.751703	11.78922	0.00181
53550.654537	11.83375	0.00143
53551.609534	11.81601	0.00173
53573.602135	11.82109	0.00367
53574.531691	11.81516	0.00241
53575.546089	11.80329	0.00211
53576.546067	11.80878	0.00268
53578.665360	11.75643	0.00232
53861.783012	11.78616	0.00224
53862.741865	11.77693	0.00231
53863.749757	11.78931	0.00313
53864.742775	11.80499	0.00315
53865.771405	11.81063	0.00170
53866.724997	11.81256	0.00223
53867.778590	11.82035	0.00119
53868.748140	11.82455	0.00114
53870.593760	11.82535	0.00148
53871.786449	11.80792	0.00085
53882.713288	11.79242	0.00154
53887.717218	11.78144	0.00173
53889.679215	11.79304	0.00290
53920.603556	11.35688	0.00264
53945.583464	11.66717	0.00125
54143.897228	11.59350	0.00227
54166.891741	11.77823	0.00367
54168.883742	11.80202	0.00200
54172.857726	11.79734	0.00192
54174.848564	11.81779	0.00196
54194.917474	11.79477	0.00173
54199.899854	11.76678	0.00205
54202.889292	11.73950	0.00190
54229.719267	11.33710	0.00368
54234.652538	11.40673	0.00257
54253.744628	11.65247	0.00399
54254.678126	11.66130	0.00275
54255.722560	11.67890	0.00264
54259.725812	11.70184	0.00340
54261.794683	11.70275	0.00901
54313.620619	11.64514	0.00232
54315.497608	11.61620	0.00129
54316.611584	11.59821	0.00156
54317.496297	11.55722	0.00083
54319.542744	11.49931	0.00102
54320.580289	11.47979	0.00111
54323.537296	11.43111	0.00138
54346.502395	11.50437	0.00253
54347.501198	11.51593	0.00267
54349.526984	11.54072	0.00226
54523.859926	11.57233	0.00254
54528.878747	11.46067	0.00303
54547.759621	11.43022	0.00186
54548.852149	11.44839	0.00269
54550.842175	11.48418	0.00210
54552.800759	11.50967	0.00233
54553.821042	11.51551	0.00226
54556.798027	11.56205	0.00186
54568.811680	11.70450	0.00172
54582.623731	11.78479	0.00284
54609.642688	11.84143	0.00040
54637.784021	11.37846	0.00708
54643.725606	11.35829	0.00136
54648.688288	11.41413	0.00140

Table 8. Radial velocity values for HD 153950.

JD-2400000.	Radial Vel. [km s ⁻¹]	Uncertainty [km s ⁻¹]
52852.541834	33.18472	0.00154
52854.596492	33.18828	0.00225
53506.793032	33.29144	0.00381
53831.893340	33.18043	0.00164
53832.896004	33.17858	0.00178
53833.897869	33.17967	0.00263
53836.894963	33.18310	0.00160
53860.919573	33.19229	0.00247
53863.788490	33.17988	0.00251
53886.726351	33.17567	0.00124
53921.606991	33.18949	0.00163
53944.556842	33.20589	0.00119
53976.479331	33.24768	0.00128
53980.560756	33.25030	0.00255
54167.860472	33.23714	0.00234
54169.858171	33.23668	0.00264
54173.850015	33.24419	0.00195
54196.826071	33.22742	0.00148
54199.882018	33.22591	0.00144
54200.808656	33.22309	0.00185
54201.910735	33.22244	0.00109
54202.795181	33.22726	0.00197
54226.886058	33.22130	0.00430
54227.810261	33.20965	0.00199
54228.798529	33.21562	0.00169
54229.766644	33.22080	0.00196
54230.838756	33.21925	0.00146
54231.794935	33.20842	0.00157
54232.713425	33.21465	0.00229
54233.903107	33.21937	0.00230
54234.783932	33.21295	0.00165
54253.698720	33.20385	0.00265
54254.731349	33.20359	0.00161
54258.659591	33.20899	0.00227
54260.837471	33.21031	0.00308
54313.649435	33.19161	0.00183
54349.550815	33.18406	0.00353
54393.493188	33.18317	0.00155
54526.824653	33.31645	0.00225
54530.902047	33.32334	0.00145
54547.786305	33.31122	0.00178
54548.903849	33.31512	0.00259
54554.855275	33.30989	0.00178
54582.757801	33.29154	0.00245
54588.928823	33.28545	0.00336
54609.734744	33.27785	0.00211
54612.769428	33.27880	0.00121
54637.793172	33.26491	0.00103
54643.794707	33.25740	0.00139